

PAPER • OPEN ACCESS

## Eu-induced lattice vibrations in $\text{Gd}_2\text{O}_3$ crystals

To cite this article: A N Kislov and A F Zatsepin 2019 *J. Phys.: Conf. Ser.* **1391** 012018

View the [article online](#) for updates and enhancements.



**IOP | ebooks™**

Bringing together innovative digital publishing with leading authors from the global scientific community.

Start exploring the collection—download the first chapter of every title for free.

# Eu-induced lattice vibrations in $\text{Gd}_2\text{O}_3$ crystals

A N Kislov<sup>1</sup> and A F Zatsepin

Institute of Physics and Technology, Ural Federal University, 19 Mira Street,  
Ekaterinburg, 620002, Russia

E-mail: a.n.kislov@urfu.ru

**Abstract.** The effect of trivalent Eu impurity occupying a position with the  $S_6$  site symmetry in cubic  $\text{Gd}_2\text{O}_3$  on the latter's structure and phonon spectrum is investigated. This study was performed by means of computer modeling within a shell model. The equilibrium structures and phonon local symmetrized densities of states were calculated. In addition, frequencies of localized vibrations induced by Eu ion were determined. The calculated results were compared with the available experimental data in literature.

## 1. Introduction

Gadolinium oxide ( $\text{Gd}_2\text{O}_3$ ) is one of the representatives of a group that consists of 17 sesquioxides of rare earths with different atomic numbers. Gadolinium sesquioxide is a material with wide technological applications ranging from magnetic to optoelectronic and nuclear fields [1]. It can be used in monocrystalline or powder and nanosized states as well as in thin-film form. A structural phase diagram for the lanthanide sesquioxides shows that at temperatures below approximately 1200°C single  $\text{Gd}_2\text{O}_3$  crystal exists in a cubic C-type phase. This crystalline phase has the bixbyite structure with space group Ia-3. In the following, we will consider only cubic  $\text{Gd}_2\text{O}_3$ .

Physical properties of defect-free gadolinium oxide such as structural [2–8], electronic [6–8], vibrational [9–12], thermodynamical [13] have been thoroughly studied both experimentally and theoretically. Additionally, various properties of  $\text{Gd}_2\text{O}_3$  doped with rare earth elements have been studied too, for example in [14–16]. It is worth noting that rare earth-doped  $\text{Gd}_2\text{O}_3$  crystals are promising systems that are used in solid-state lasers, display devices, etc.

Over the last few decades, interest in europium-doped  $\text{Gd}_2\text{O}_3$  has grown considerably due to specific photoluminescence properties [17–20]. Less attention has been paid to the study of the lattice strain and vibrational properties of  $\text{Gd}_2\text{O}_3$  doped with europium ( $\text{Eu}^{+3}$ ). Meanwhile, a comprehensive description of the dynamic processes in  $\text{Gd}_2\text{O}_3$ -based materials is impossible without knowledge about localized vibrations caused by defects. The microscopic mechanisms of the processes taking place are still not fully understood. In the present paper, we focus on the investigation of local atomic structures and defect vibrations of  $\text{Gd}_2\text{O}_3$  with trivalent Eu substitutional impurities which occupy Wyckoff 8b positions with the  $S_6$  symmetry.

## 2. Computational Procedures

The lattice structure of  $\text{Gd}_2\text{O}_3$  containing Eu impurities and frequencies of localized vibrations due to these impurities were calculated within the framework of a cluster approach [21]. The crystal is

<sup>1</sup> E-mail address: a.n.kislov@urfu.ru.



divided into an inner spherical region containing the defect and an outer region with the remaining ions. The inner region is large enough. In this region interactions between atoms are considered at a microscopic level. Outer region is treated in the approximation of a polarizable continuum and extends to infinity.

To describe the interatomic interactions we used the realistic shell model [22]. This ionic model takes into account the long-range Coulomb interaction between cores and the interaction between shells, the potential of which consists of two parts: the Coulomb term and the short-range term. The short-range potential used here is the Buckingham potential with parameters proposed by Lewis [23]. It was shown that, with the this potential, the calculated lattice constant of 10.721 Å, bulk modulus of 161.7 GPa and heat capacity of 101.0 J K<sup>-1</sup> mol<sup>-1</sup> for perfect gadolinium oxide are in good agreement with the experimental data of 10.817 Å [4], 117.6 GPa [24] and 105.5 J K<sup>-1</sup> mol<sup>-1</sup> [13], respectively.

The structure optimization of Gd<sub>2</sub>O<sub>3</sub>:Eu was performed through minimizing the lattice energy. For this we have employed the lattice static method [25]. The local energy minimum was achieved iteratively using the Newton–Raphson matrix method. The inverse matrix of second derivatives of the energy was updated at each iteration based upon BFGS method.

An analysis of local symmetrized densities of states (LSDOS) of phonons in perfect Gd<sub>2</sub>O<sub>3</sub> and defective Gd<sub>2</sub>O<sub>3</sub>:Eu made it possible to estimate the effect of Eu<sup>+3</sup> ions on the vibrational spectrum and to define the frequencies of localized vibrations. The method, which has been used for the calculation of these LSDOS, is the recursion method [26], which is rather efficient. The first step of the recursion method is to select the initial vector of the vibrational state of an appropriate symmetry. The projection operator method was applied to determine the symmetry coordinates of this starting vector.

### 3. Results and Discussion

#### 3.1. Local atomic structure

First, we consider the lattice structure of perfect Gd<sub>2</sub>O<sub>3</sub> crystals. Our calculations show that Gd1 ion located at the S<sub>6</sub> site is bonded to six O ions at 2.312 Å. These oxygens form first coordination shell (see figure 1). Six nearest Gd2 ions located at C<sub>2</sub> sites form second coordination shell at a distance of 3.576 Å. These data are close to those obtained earlier the extended X-ray absorption fine structure method [7].

In Eu-doped Gd<sub>2</sub>O<sub>3</sub>, the distances between Eu<sup>+3</sup> ion and nearest ions are found to be greater than bond lengths in the defect-free crystal. The calculated results of distances between some ions are listed in Table 1. Unfortunately, the authors do not know experimental data on the structure of cubic Gd<sub>2</sub>O<sub>3</sub> when Gd<sup>+3</sup> ions are replaced by Eu<sup>+3</sup> ions. However, the obtained values are in good agreement with the fact that the Gd<sup>+3</sup> ionic radius (0.94 Å) is slightly less than Eu<sup>+3</sup> ion (0.95 Å).

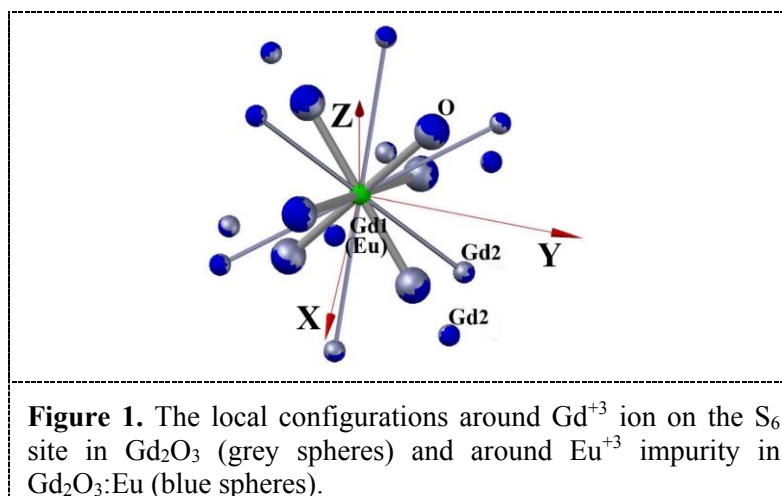


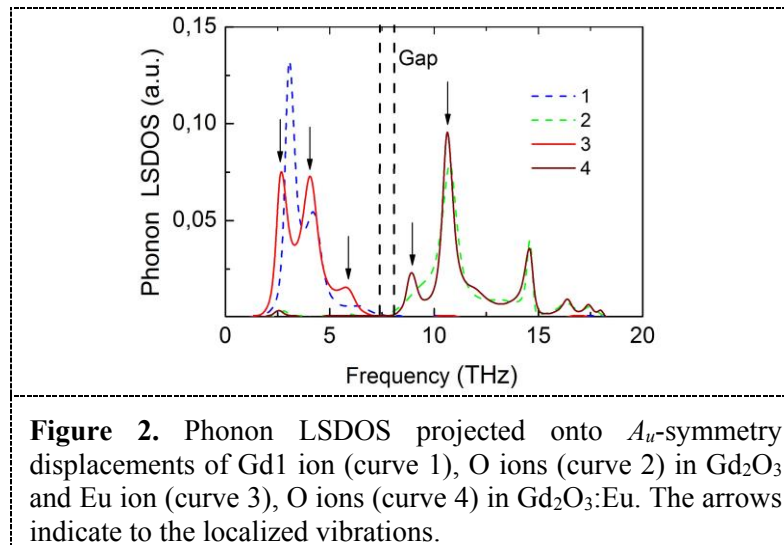
**Table 1.** Interionic distances (Å) for  $\text{Gd}_2\text{O}_3$  and  $\text{Gd}_2\text{O}_3:\text{Eu}^{+3}$ .

Ions	Coordination number	$\text{Gd}_2\text{O}_3$		$\text{Gd}_2\text{O}_3:\text{Eu}^{+3}$
		This work	Expt.[7]	This work
Gd1[or Eu]–O	6	2.312	2.308	2.320
Gd1[or Eu]–Gd2	6	3.576	3.570	3.580
Gd1[or Eu]–Gd2	6	4.017		4.019

### 3.2. Vibrational Dynamics for $\text{Gd}_2\text{O}_3:\text{Eu}$

Since  $\text{Gd}^{+3}$  and  $\text{Eu}^{+3}$  ions in  $\text{Gd}_2\text{O}_3$  and  $\text{Gd}_2\text{O}_3:\text{Eu}$  crystals is surrounded by six  $\text{O}^{2-}$  ions as nearest neighbors, the phonon LSDOS projected onto ion vibrational displacements of  $\text{GdO}_6$  and  $\text{EuO}_6$  units have been calculated.  $\text{O}^{2-}$  ions participate in the vibrations of the  $A_g$ -,  $A_u$ -,  $E_g$ - and  $E_u$ -symmetries. Vibrational symmetry modes in which the motion of  $\text{Gd}^{+3}$  and  $\text{Eu}^{+3}$  ions is involved are under the representations of  $A_u$  and  $E_u$ .

For example, figure 2 shows the phonon LSDOS projected onto  $A_u$ -symmetry displacements of Gd1 ion and O ions in  $\text{Gd}_2\text{O}_3$  and Eu ion and O ions in  $\text{Gd}_2\text{O}_3:\text{Eu}$ . According to our calculations  $\text{Gd}^{+3}$  and  $\text{Eu}^{+3}$  ion motions dominate up to 7 THz. Oxygen movement plays a great role at the high frequencies above 8 THz. When Eu impurity is created, the low-frequency band of the phonon density is shifted to the low-frequency part of the spectrum. The frequencies of localized symmetrized vibrations induced by Eu impurity are summarized in Table 2.

**Table 2.** Frequencies (THz) of localized vibrations in  $\text{Gd}_2\text{O}_3$  with  $\text{Eu}^{+3}$  on the position 8b.

Ions	Mode	Vibration symmetry			
		$A_g$	$A_u$	$E_g$	$E_u$
Eu			2.6, 4.2, 6.2		2.6, 4.4, 6.6
O	stretching	10.8, 16.8, 17.6	8.8, 10.6	8.6, 10.8, 12.6, 13.8	9.0, 11.4, 14.4
	bending	10.4, 12.2, 14.4, 17.6	8.6, 10.8, 14.4	8.4, 10.6, 14.6, 16.2, 16.8, 17.6	8.6, 10.8, 12.2, 14.4

#### 4. Conclusion

In summary, we have successfully simulated the local atomic structure and phonon LSDOS for the cubic  $\text{Gd}_2\text{O}_3$  crystal with trivalent Eu impurities occupying  $S_6$  crystallographic sites. The calculations were carried out within a shell model, the reliability of which is confirmed by the good agreement between the calculated and measured data for some physical quantities of perfect  $\text{Gd}_2\text{O}_3$ .

The simulation predicts an increase in the distances between Eu ion and nearest ions as compared to bond lengths in the perfect crystal. The lattice dynamics calculations allowed to determine the frequencies of Eu impurity-induced vibrations in  $\text{Gd}_2\text{O}_3\text{:Eu}$ .

#### Acknowledgments

The work was supported partially by the Ministry of Education and Science of the Russian Federation (Government Task № 3.1485.2017/4.6) and by Act 211 of Government of the Russian Federation, contract № 02.A03.21.0006.

#### References

- [1] Qadri S B, Wu D H, Bussman K and Qadri S N 2015 *Phys. Status Solidi B* **252** 2020
- [2] Bartos A, Lieb K P, Uhrmacher M and Wiarda D 1993 *Acta Cryst. B* **49** 165
- [3] Hirosaki N, Ogata S and Kocer C 2003 *J. Alloy. Compd.* **351** 31
- [4] Kennedy B J and Avdeev M 2011 *Aust. J. Chem.* **64** 119
- [5] Jamnezhad H and Jafari M J. 2016 *Magn. and Magn. Mater.* **408** 164
- [6] Doi K, Fujitani K, Kadowaki N, Nakamura K, Tachibana A and Hattori T 2005 *Jpn. J. Appl. Phys.* **44** 6115
- [7] Perevalov T V, Dolbak A E, Shvets V A, Gritsenko V A, Asanova T I and Erenburg S B 2014 *Eur. Phys. J. Appl. Phys.* **65** 10702
- [8] Jamnezhad H and Jafari M 2017 *J. Comput. Electron.* **16** 272
- [9] Bloor D and Dean J R 1972 *J. Phys. C: Solid State Phys.* **5** 1237
- [10] Le Luyer C, Garcia-Murillo A, Bernstein E and Mugnier J 2003 *J. Raman Spectrosc.* **34** 234
- [11] Jinqui Y U, Lei C U I, Huaqiang H E, Shihong Y A N, Yunsheng H U and Hao W U 2014 *J. Rare Earths* **32** 1
- [12] Abrashev M V, Todorov N D and Geshev J 2014 *J. Appl. Phys.* **116** 103508
- [13] Zinkevich M 2007 *Prog. Mater. Sci.* **52** 597
- [14] Buijs M, Meyerink A and Blasse G 1987 *J. Lumin.* **37** 9
- [15] Krizan J, Mazaj M, Kaucic V, Bajsic I and Mozina J 2014 *Acta Chim. Slov.* **61** 608
- [16] Liu Y, Liu G, Wang J, Dong X and Yu W 2015 *J. Alloy. Compd.* **649** 96
- [17] Wang Y, Milosevic O, Gomez L, Rabanal M E, Torralba J M, Yang B and Townsend P D 2006 *J. Phys.: Condens. Matter.* **18** 9257
- [18] Iwako Y, Akimoto Y, Omiya M, Ueda T and Yokomori T 2010 *J. Lumin.* **130** 1470
- [19] Choi S, Park B-Y, Ahn T, Kim J Y, Hong C S, Yi M H and Jung H-K 2011 *Thin Solid Films* **519** 3272
- [20] Alammar T, Cybinska J, Campbell P S and Mudring A V 2016 *J. Lumin.* **169** 587
- [21] Kislov A N 2004 *Zinc Oxide – A Material for Micro- and Optoelectronic Applications (NATO Science Series vol 194)* ed N H Nickel and E Terukov (Amsterdam: Kluwer Academic Publishers) pp 183–194
- [22] Dick B G and Overhauser A W 1958 *Phys. Rev.* **112** 90
- [23] Lewis G V and Catlow C R A. 1985 *J. Phys. C: Solid State Phys.* **18** 1149
- [24] Lonappan D, Shekar N V C, Sahu P C, Kumarasamy B V, Bandyopadhyay A K and Rajagopalan M 2008 *Philos. Mag. Letters* **88** 47
- [25] Richardson D D 1982 *Comp. Phys. Commun.* **28** 75
- [26] Meek P E 1976 *Philos. Mag.* **33** 897